Check for updates

One-pot enzymatic synthesis of L-threitol from C1 formaldehyde†

Sanrunyi Gong,‡[a] Tianzhen Li,‡[b,c] Zijing Tang,[c] Zijian Tan,[c,d] Ruke Zhang,[c] Karsten Olsen,[e] Haifeng Liu [ID] *[d] and Leilei Zhu [ID] *[c]

Here, we report an enzymatic cascade reaction converting a high concentration of formaldehyde into L-threitol. The cascade reaction starts with the carboligation of formaldehyde catalyzed by formolase and fructose-6-phosphate aldolase, generating L-erythrulose. Subsequently, a newly identified L-threitol dehydrogenase facilitates the conversion of L-erythrulose into L-threitol, utilizing NADH as a coenzyme. Three types of NADH regeneration systems were investigated to facilitate the recycling of NADH in the reaction system. 405.7 mM (49.6 g L^{-1}) L-threitol was achieved from the conversion of formaldehyde in a one-pot reaction system with a self-sufficient NADH recycling system, which is based on the oxidation of glycerol catalyzed by glycerol dehydrogenase. Furthermore, the highest yield (89.4%; 251.3 mM) of L-threitol from formaldehyde was achieved in the one-pot two-step reaction system in which NADH was efficiently recycled by using methanol dehydrogenase and isopropanol.

Green foundation

1. Current synthetic approaches for L-threitol face challenges in producing high purity L-threitol from affordable raw materials under mild reaction conditions. The enzymatic cascade reaction designed in this study converts the renewable resource formaldehyde into L-threitol at mild temperature with trivial side products, presenting a green and promising strategy for L-threitol production.

2. Compared to the harsh chemicals and energy-intensive conditions used in chemical L-threitol synthesis, this study provides an enzymatic synthesis method for L-threitol, which is performed at 30 °C and pH 7.4 and produces trivial side products.

3. The four enzymes involved in this cascade reaction require further enhancement in their enzymatic properties, *e.g.* activity and stability, to further increase the productivity, yield and overall cost. Systematic optimization of the reaction conditions would be beneficial for performing the conversion of formaldehyde into L-threitol on a larger scale.

[a]*Sino-Danish College, University of Chinese Academy of Sciences, Beijing 100049, China*

[b]*Haihe Laboratory of Synthetic Biology, 21 West 15th Avenue, Tianjin Airport Economic Area, Tianjin 300308, China*

[c]*State Key Laboratory of Engineering Biology for Low-Carbon Manufacturing, Tianjin Institute of Industrial Biotechnology, Chinese Academy of Sciences, Tianjin 300308, China. E-mail: zhu_ll@tib.cas.cn*

[d]*Jiangsu Collaborative Innovation Centre of Chinese Medicinal Resources Industrialization, School of Pharmacy, Nanjing University of Chinese Medicine, Nanjing 210023, China. E-mail: haifeng.liu@njucm.edu.cn*

[e]*Department of Food Science, University of Copenhagen, Frederiksberg C, Denmark*

†Electronic supplementary information (ESI) available. See DOI: https://doi.org/10.1039/d4gc05638h

‡These authors contributed equally.

L-Threitol is a four-carbon sugar alcohol with significant biotechnological applications. In the pharmaceutical industry, L-threitol serves as a key intermediate for the production of anticancer drugs like treosulfan, interferon-gamma interleukin-4, threitol ceramide (ThrCer$_2$) and *tert*-butyrate ester.[1–3] L-Threitol is also a precursor for the synthesis of various chiral compounds, including chiral macrocyclic dianhydrides and 1,4-di-*O*-benzyl threitol.[4,5] Its ability to serve as a building block for synthetic phospholipids and other artificial amphiphilic phosphates highlights its importance in diverse synthesis applications.[6] Moreover, L-threitol is utilized in the production of oxygen-sensitive pigments, contributing to the

development of intelligent plastic films used in food packaging.[7]

As depicted in Scheme 1, there are several reported synthesis routes for L-threitol. L-Threitol can be synthesized by converting 1,3-butadiene through a dihydroxylation reaction using OsO_4 as the catalyst (Scheme 1a).[8] L-Threitol can also be synthesized by converting unprotected glycolaldehyde using a $Zn(Pro)_2$ complex as the catalyst (Scheme 1b).[9] Moreover, L-threitol can be produced from the reduction of L-tartaric acid (Scheme 1c), which requires high pressure H_2 and elevated temperatures (150 °C).[10] However, erythritol and D-threitol were also generated as side products with the above-mentioned

chemical methods, which require fastidious purification procedures. Biotransformation strategies were also reported for the synthesis of L-threitol. Xylitol dehydrogenase derived from Guinea-pig liver was used for the first time to convert L-erythrulose to L-threitol *in vitro* (Scheme 1d). However, the conversion rate was not mentioned.[11] Furthermore, aldo-keto reductase was reported to reduce L-threose to L-threitol (Scheme 1e).[12] Overall, current synthetic approaches face challenges in producing high purity L-threitol using affordable raw materials and mild reaction conditions.
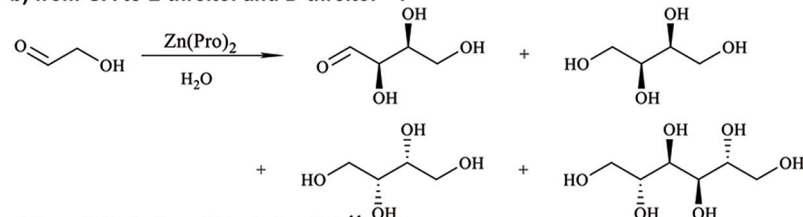
Formaldehyde, an inexpensive one-carbon substrate, can be produced in large quantities using mature technologies from
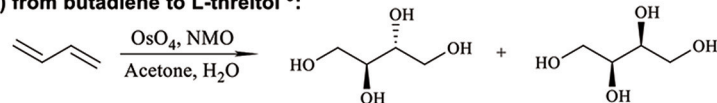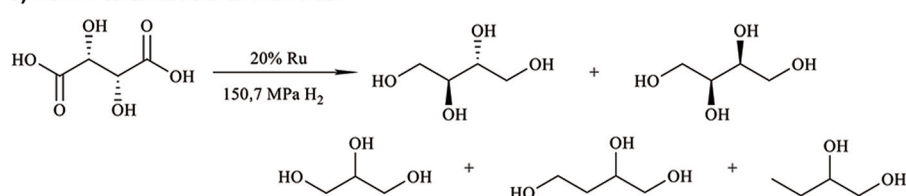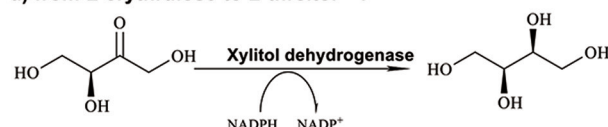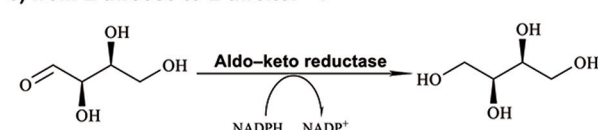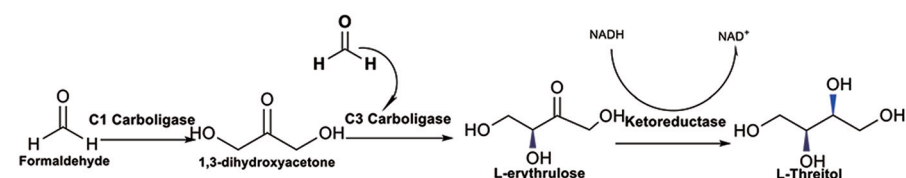

Scheme 1 Representative examples of threitol synthesis.[9–13]

renewable sources, making it an attractive feedstock for the new generation of bio-manufacturing.[13,14] Here, we present the first enzymatic synthesis of L-threitol from formaldehyde. As shown in Scheme 2, the designed cascade starts with the formolase_BFD-M6 catalyzed carboligation of formaldehyde into 1,3-dihydroxyacetone (DHA), subsequently followed by the fructose-6-phosphate aldolase FSA^A129S catalyzed condensation reaction of formaldehyde and DHA into L-erythrulose. The produced L-erythrulose was reduced to L-threitol by using L-threitol dehydrogenase as the biocatalyst and NADH as a coenzyme. Different NADH recycling strategies were further investigated and compared. The $\Delta rG'^{\circ}$ of the designed routes for L-threitol synthesis from formaldehyde was −127.5 kJ mol^{-1} under standard conditions, indicating that the designed route was thermodynamically favourable. Overall, the designed enzymatic cascade reaction converts the renewable resource formaldehyde into L-threitol under mild conditions with trivial side products, presenting a green and promising strategy for L-threitol production.

Firstly, formolase_BFD-M6 previously developed by our group was selected to catalyze the conversion of formaldehyde into DHA in the first step at 30 °C and pH 7.4, owing to its high resistance to formaldehyde and strong product specificity for C3 DHA.[13] To ensure high formaldehyde conversion, we initially used a relatively high concentration of formolase_BFD-M6 (0.13 mM). Time-point sampling over a 22 hour reaction period revealed that the production of DHA reached its maximum at 5 hours and remained stable thereafter. As shown in Fig. 1A, when increasing the concentration of formaldehyde from 300 mM to 2100 mM, the maximum yield of DHA (302.13 mM) was obtained with 1200 mM formaldehyde as the substrate (Fig. 1A). For the second step, D-fructose-6-phosphate aldolase FSA^A129S [15,16] was used to convert DHA and formaldehyde into C4 L-erythrulose. To efficiently convert the substrate, formaldehyde, a one-step enzymatic process involving
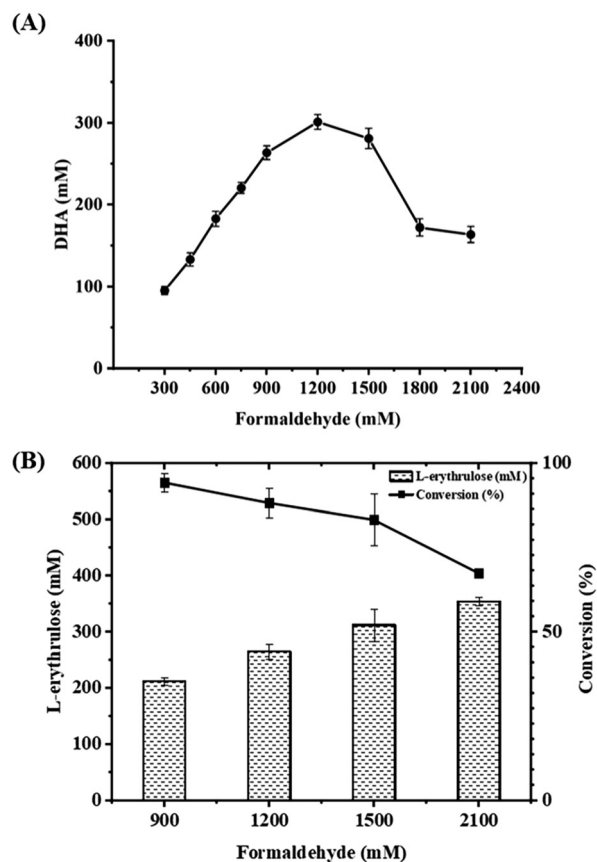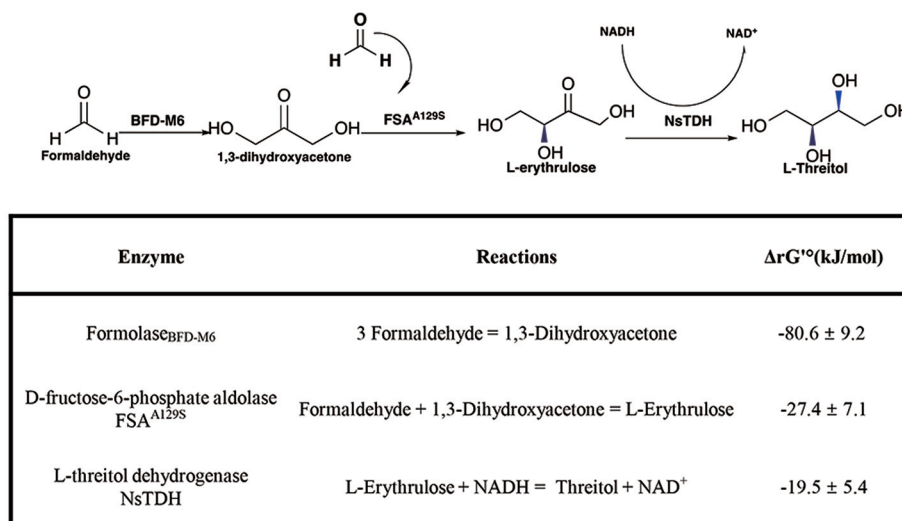

Fig. 1 (A) Performance of 0.13 mM formolase_BFD-M6 at varied concentrations of formaldehyde in 5 h. (B) The catalytic synthesis of L-erythrulose from varied concentrations of formaldehyde was performed using 0.13 mM formolase_BFD-M6 and 0.33 mM FSA^A129S for 6 h. The reactions were performed in a phosphate buffer (50 mM potassium phosphate, 5 mM MgSO$_4$, pH 7.4) containing 1 mM TPP, with shaking at 1000 rpm and 30 °C. The enzymes in the reaction were removed using a 3 kDa Millipore ultrafiltration membrane prior to product detection by HPLC.

Enzyme	Reactions	$\Delta rG'^{\circ}$(kJ/mol)
Formolase_BFD-M6	3 Formaldehyde = 1,3-Dihydroxyacetone	-80.6 ± 9.2
D-fructose-6-phosphate aldolase FSA^A129S	Formaldehyde + 1,3-Dihydroxyacetone = L-Erythrulose	-27.4 ± 7.1
L-threitol dehydrogenase NsTDH	L-Erythrulose + NADH = Threitol + NAD$^+$	-19.5 ± 5.4

Scheme 2 Enzymatic cascade reaction for the synthesis of L-threitol from formaldehyde. Standard Gibbs energy change ($\Delta rG'^{\circ}$) was calculated by using eQuilibrator (pH 7.4, ionic strength 0.05 M). $\Delta rG'$ was calculated based on the actual reaction conditions of Fig. 1B, as shown in Table S1.†

formolase$_{BFD-M6}$ and FSA^{A129S} was carried out. Thermodynamic analysis showed that coupling these two enzymatic reactions results in a pulling effect which enables rapid conversion of formaldehyde in the system. For the subsequent pulling reaction to convert DHA to L-erythrulose, a higher concentration of FSA^{A129S} (0.33 mM) was employed. As a pH of 7.5 was reported for the coupled catalysis by formolase and FSA^{A129S} in a previous study,[15] we conducted the coupled reactions under the same temperature (30 °C) and pH (7.4) conditions as those used for the initial reaction catalyzed by formolase$_{BFD-M6}$. As shown in Fig. 1B, the highest conversion of 94.2% was obtained with 900 mM formaldehyde, yielding 211.94 mM L-erythrulose. At a formaldehyde concentration of 2100 mM, the highest yield of L-erythrulose reached 353.68 mM with a corresponding conversion of 67.35%.

The key enzyme in the third step of the reaction route is L-threitol dehydrogenase for the reduction of L-erythrulose into L-threitol. L-Threitol dehydrogenase with strict substrate prefer-ence towards L-erythrulose is required for the construction of the cascade reaction. Few enzymes have been reported to catalyze the reduction of L-erythrulose to L-threitol. Erythritol/L-threitol dehydrogenase (EltD) from *Mycobacterium smegmatis* was reported to be able to convert L-erythrulose to L-threitol.[17] However, EltD can also convert D-erythrulose, D-xylulose, L-xylulose and ribulose to the corresponding sugar alcohol, which interferes with the designed cascade reaction of this study. It was reported that xylitol dehydrogenase from *Gluconobacter oxydans* (GoXDH) irreversibly converted L-erythrulose to erythritol at pH 8.[18] Phylogenetic analysis of L-threitol dehydrogenase was therefore performed using GoXDH as a template. There were 232 genes with a homology of 40%–70% from the NCBI BLAST (**https://blast.ncbi.nlm.nih.gov/Blast.cgi**) available for phylogenetic analysis. The phylogenetic tree (Fig. S1†) was constructed with approximately maximum-likelihood methods using the software MEGA11. After conducting a thorough analysis and aligning
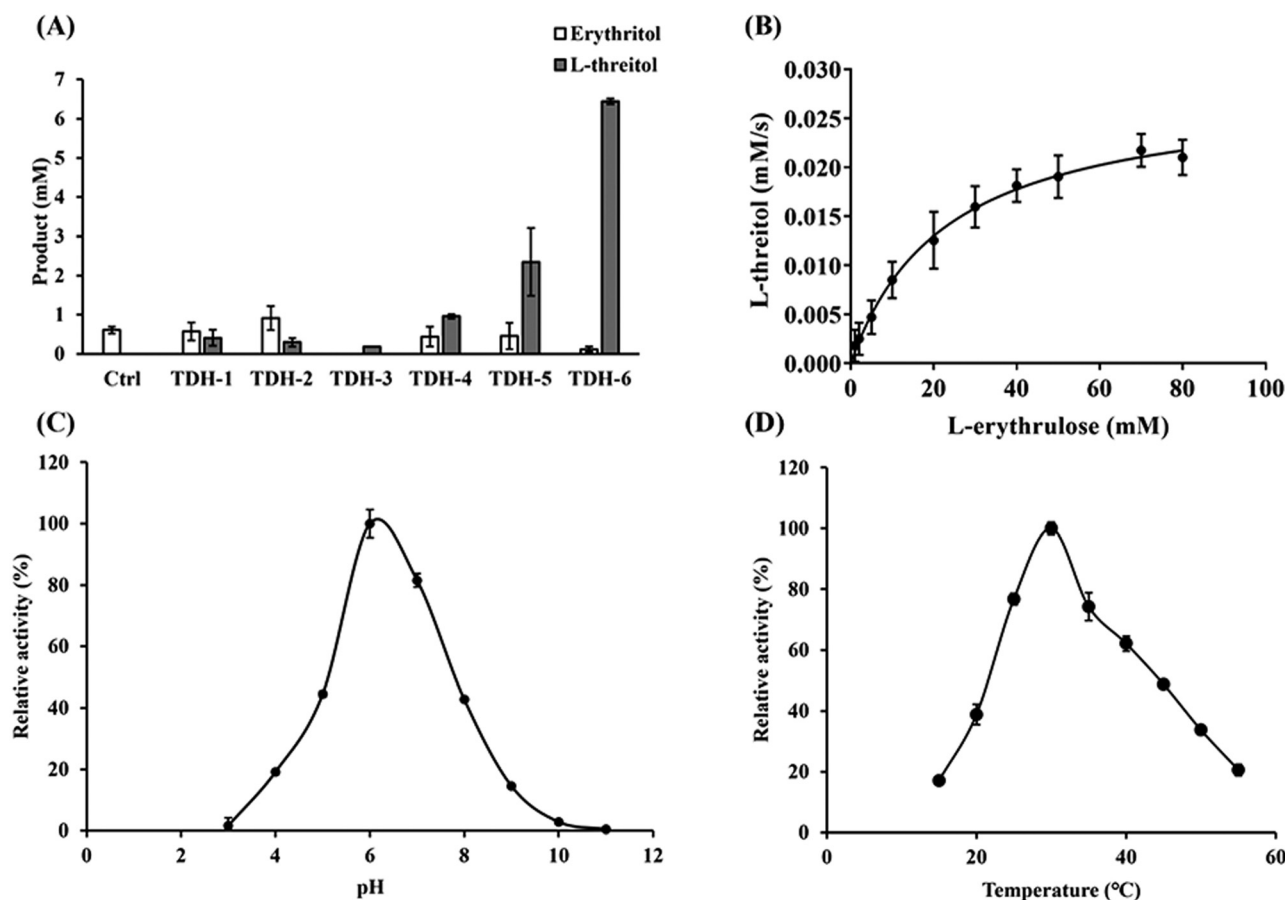

Fig. 2 Identification and enzymatic characterization of L-threitol dehydrogenase. (A) Six candidate L-threitol dehydrogenases were identified functionally and pET28a was added to the control group. (B) Kinetics curve of L-threitol dehydrogenase NsTDH at 30 °C. (C) The pH profile of L-threitol dehydrogenase NsTDH. The following buffers were used: citric acid buffer (50 mM citric acid and trisodium citrate dihydrate, 5 mM MgSO$_4$) with different pH values (3.0, 4.0, and 5.0), phosphate buffer (50 mM potassium phosphate, 5 mM MgSO$_4$) with different pH values (6.0, 7.0 and 8.0) and glycine–NaOH buffer (50 mM glycine and NaOH, 5 mM MgSO$_4$) with different pH values (9.0, 10.0, and 11.0). The reaction solution contained 50 mM buffer, 8 mM L-erythrulose, 2 mM NADH and 1.76 μM NsTDH. (D) The temperature profile of L-threitol dehydrogenase NsTDH. The reaction solution contained 50 mM potassium phosphate buffer (pH 6.0, 5 mM MgSO$_4$), 8 mM L-erythrulose, 2 mM NADH, and 1.76 μM NsTDH.

the phylogenetic tree, six amino acid sequences were chosen as potential candidates for L-threitol dehydrogenases (Table S2†). After cloning, the six candidate enzymes were successfully expressed. The activity of the six candidate enzymes was measured and compared after quantifying the L-threitol converted from 20 mM L-erythrulose. As shown in Fig. 2A, TDH-6 from *Nostoc sp.* (named NsTDH) showed the highest activity and therefore was selected for the conversion

of L-erythrulose to L-threitol in the synthesis route. The enzymatic properties of the L-threitol dehydrogenase NsTDH were investigated further after purification. The apparent kinetic constants of NsTDH were determined to be 15.72 s^{-1} for k_{cat} and 23.09 mM for K_m, respectively. Furthermore, the optimum pH for the reduction of L-erythrulose and the optimum temperature of NsTDH were determined to be pH 6.0 and 30 °C, respectively (Fig. 2).
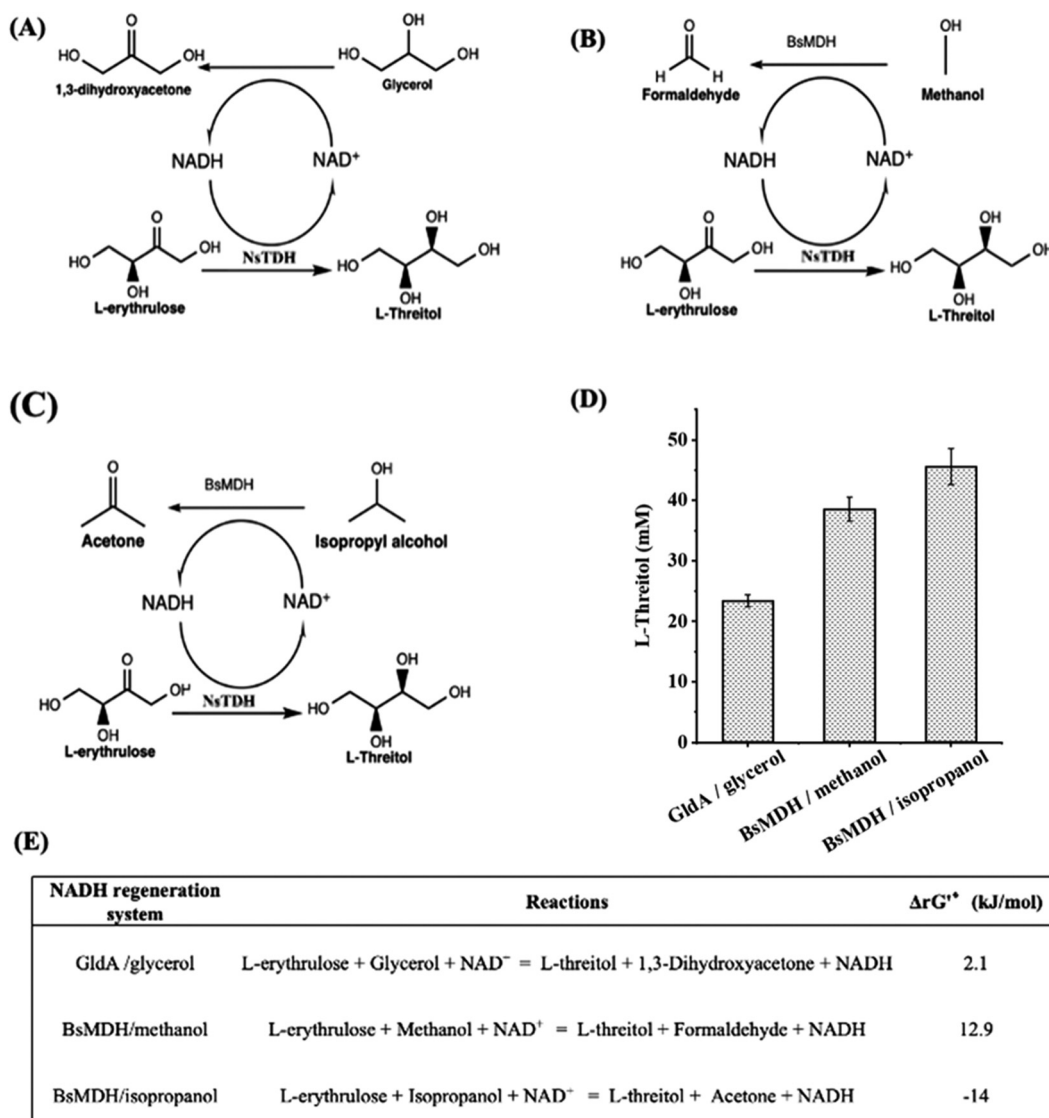

Fig. 3 Reduction of L-erythrulose to L-threitol with different NADH regeneration systems. (A) NADH regeneration system using GldA/glycerol. (B) NADH regeneration system using BsMDH/methanol. (C) NADH regeneration system using BsMDH/isopropanol. (D) Reduction of L-erythrulose to L-threitol with different NADH regeneration systems. The GldA/glycerol NADH regeneration system solution contained 75 mM L-erythrulose, 75 mM glycerol, 2 mM NADH, 0.11 mM NsTDH and 0.15 mM GldA. The BsMDH/methanol NADH regeneration system solution contained 75 mM L-erythrulose, 75 mM methanol, 2 mM NADH, 0.11 mM NsTDH and 0.14 mM BsMDH. The BsMDH/isopropanol NADH regeneration system solution contained 75 mM L-erythrulose, 75 mM isopropanol, 2 mM NADH, 0.11 mM NsTDH and 0.14 mM BsMDH. All systems were prepared in 50 mM potassium phosphate buffer (pH 7.4) containing 5 mM MgSO$_4$ and incubated at 30 °C with shaking at 1000 rpm in a 1.5 mL microcentrifuge tube for 14 h. (E) Standard Gibbs energy change ($\Delta rG'°$) of individual reactions for L-threitol production. The $\Delta rG'°$ were calculated by using eQuilibrator (https://equilibrator.weizmann.ac.il/) at pH 7.4 and an ionic strength of 0.05 M. $\Delta rG'$ was calculated based on the actual reaction conditions of (D), as shown in Table S3.†

The NsTDH-catalyzed reduction reaction requires cofactor NADH. Therefore, glycerol dehydrogenase (GldA) from *Escherichia coli*[19] and methanol dehydrogenase (BsMDH) from *Bacillus stearothermophilus*[20] were investigated for the recycling of NADH. When using the GldA/glycerol system, NAD$^+$ was reduced to NADH while glycerol was oxidized into DHA (Fig. 3A), which can be carboligated with formaldehyde by FSA^{A129S}, producing L-threitol. When using the BsMDH/methanol system, NADH was regenerated while methanol got oxidized into formaldehyde (Fig. 3B). The generated formaldehyde could be further used as a substrate to produce L-threitol. When using the BsMDH/isopropanol system, NADH was regenerated while isopropanol was oxidized into acetone (Fig. 3C). In principle, the generated acetone could be further recovered by evaporation. To optimize enzyme concentrations for efficient NADH regeneration, 0.1–0.15 mM GldA were tested in the GldA/glycerol system, while 0.08 and 0.14 mM BsMDH were tested in the BsMDH/methanol and BsMDH/isopropanol systems. As shown in Fig. S2,† the highest yield of L-threitol in the GldA/glycerol system was achieved at 0.15 mM GldA. In the BsMDH/methanol and BsMDH/isopropanol systems, the yield of L-threitol showed little difference between 0.08 and 0.14 mM BsMDH; thus, 0.14 mM BsMDH was used in subsequent experiments. These systems facilitated efficient NADH recycling and the utilization of oxidized intermediates, enhancing substrate conversion for L-threitol production. As shown in Fig. 3D, the NADH regeneration systems using GldA/glycerol, BsMDH/methanol and BsMDH/isopropanol yielded 23.4 mM, 38.5 mM and 45.6 mM L-threitol from 75 mM L-erythrulose, respectively. The maximum conversion among the three systems was 60.8%. From the thermodynamic perspective, the BsMDH/isopropanol NADH regeneration system is the most favourable one (Fig. 3E). From the atom economy aspect, both the GldA/glycerol NADH regeneration system and the BsMDH/methanol NADH regeneration system are preferred. Subsequently, all three systems were investigated further for the conversion of formaldehyde into L-threitol.

After evaluating the coenzyme recycling modules, the three NADH regeneration systems were incorporated into the L-threitol synthesis pathway for one-pot synthesis from formaldehyde. Based on the L-erythrulose yield catalyzed by formolase$_{BFD-M6}$ and FSA^{A129S} in the first two reactions (Fig. 1B) and the maximum conversion of 61% for L-erythrulose to L-threitol (Fig. 3D), slightly higher concentrations of methanol and isopropanol (170, 220, 280 and 380 mM) than the theoretical NADH demands (130, 161, 190, and 216 mM) were used in the BsMDH/methanol and BsMDH/isopropanol systems to ensure sufficient NADH regeneration. For the GldA/glycerol system, significantly higher concentrations of glycerol were used to enhance NADH regeneration and provide additional reducing power for L-erythrulose production. As shown in Fig. 4A, with the increase of formaldehyde and glycerol in the system, the yield of L-threitol increased gradually. 405.7 mM (49.6 g L^{-1}) of L-threitol was achieved with 1200 mM formaldehyde and 600 mM glycerol, and the yield of L-threitol reached 54.09% (Fig. 4B). 18.1 mM
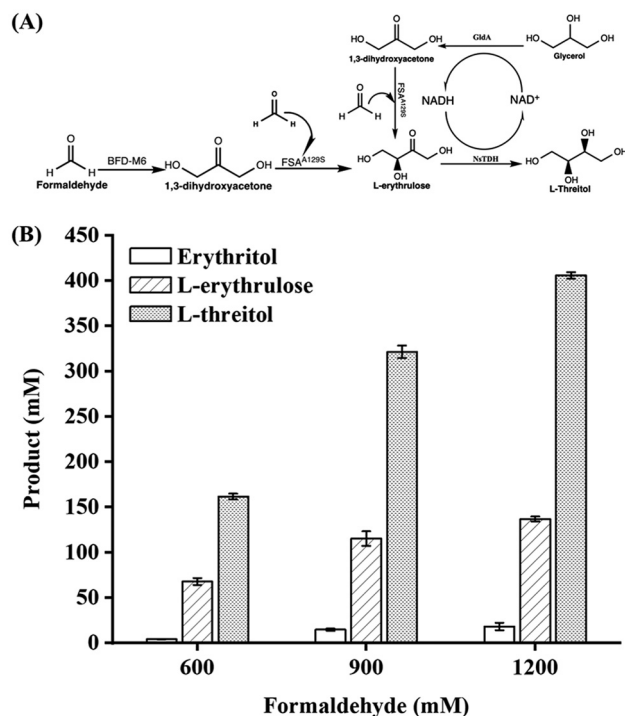

Fig. 4 One-pot synthesis of L-threitol from formaldehyde using the GldA/glycerol system for NADH regeneration. (A) The reaction route for L-threitol synthesis using the GldA/glycerol system for NADH regeneration. (B) The yield of L-threitol at different concentrations of formaldehyde. L-Threitol was produced using 0.5 mL standard reaction solution containing 50 mM phosphate buffer (50 mM potassium phosphate, 5 mM MgSO$_4$, pH 7.4), 1 mM TPP, 2 mM NAD$^+$, 0.13 mM formolase$_{BFD-M6}$, 0.26 mM FSA^{A129S}, 0.15 mM GldA, 0.11 mM NsTDH, and different concentrations of formaldehyde (600, 900 and 1200 mM formaldehyde with the addition of 300, 450 and 600 mM glycerol to the system, respectively). The reactions were carried out at 30 °C and 1000 rpm in a 1.5 mL microcentrifuge tube for 17 h.

erythritol and a significant accumulation of 137.05 mM L-erythrulose were observed in the final products. The generation of erythritol was likely to be caused by GldA, which can also convert L-erythrulose to both erythritol and L-threitol (Fig. S3†). The accumulation of L-erythrulose was caused by an imbalance between the consumption and production of L-erythrulose in the system. As shown in Fig. S4,† in the control group without formolase$_{BFD-M6}$, the yield of L-threitol was decreased significantly, confirming that the production of DHA from formaldehyde by formolase$_{BFD-M6}$ was critical for the production of L-threitol in the system.

Fig. 5A shows the one-pot two-step synthesis of L-threitol from formaldehyde using the BsMDH/methanol system for NADH regeneration. Methanol was used as a co-substrate to achieve NADH regeneration, converting L-erythrulose to L-threitol. When 170 mM methanol was added in the second step, 118.42 mM L-threitol was obtained. However, when 380 mM methanol was added to 2100 mM formaldehyde, the yield of L-threitol decreased to 90.18 mM (Fig. 5B). This
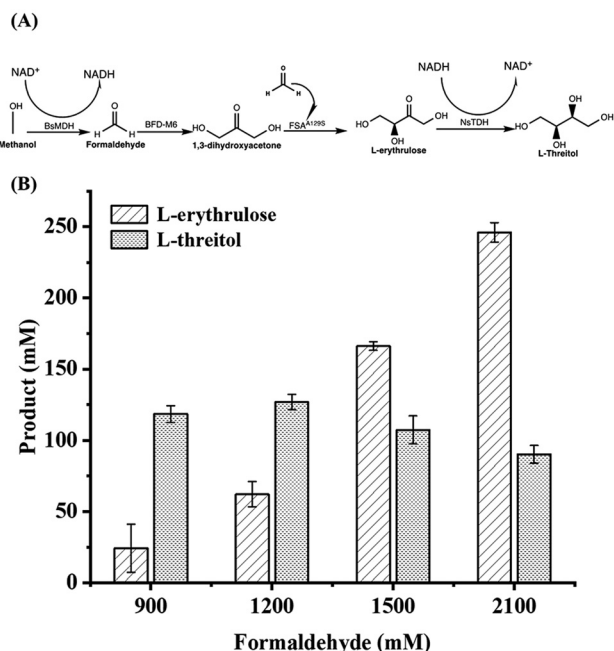
(A)

(B)

Fig. 5 One-pot two-step synthesis of L-threitol from formaldehyde using the BsMDH/methanol system for NADH regeneration. (A) The reaction route for L-threitol synthesis using the BsMDH/methanol system for NADH regeneration. (B) The yield of L-threitol at different concentrations of formaldehyde. To produce L-erythrulose, a 750 µL standard reaction mixture with potassium phosphate buffer (50 mM potassium phosphate, 5 mM MgSO$_4$, pH 7.4) containing 900, 1200, 1500 and 2100 mM formaldehyde, 0.33 mM FSA^{A129S} and 0.13 mM formolase$_{BFD-M6}$ was used in the first step. The first step was carried out at 30 °C for 8 h. Subsequently, 2 mM NADH, 0.11 mM NsTDH, 0.14 mM BsMDH and 170, 220, 280 or 380 mM methanol were added in the second step, which was performed for 12 h.
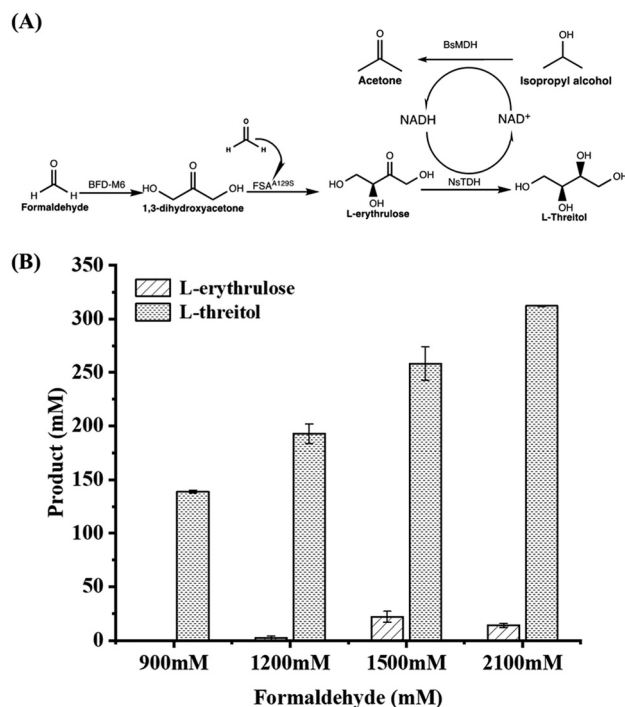
(A)

(B)

Fig. 6 One-pot two-step synthesis of L-threitol from formaldehyde using the BsMDH/isopropanol system for NADH regeneration. (A) The reaction route for L-threitol synthesis using the BsMDH/isopropanol system for NADH regeneration. (B) The yield of L-threitol at different concentrations of formaldehyde. To produce L-erythrulose, a 750 µL standard reaction mixture with phosphate buffer (50 mM potassium phosphate, 5 mM MgSO$_4$, pH 7.4) containing 900, 1200, 1500, or 2100 mM formaldehyde, 0.33 mM FSA^{A129S} and 0.13 mM formolase$_{BFD-M6}$ was used in the first step. The reactions were carried out at 30 °C with shaking at 1000 rpm in a 1.5 mL microcentrifuge tube for 8 h. Subsequently, a 1 mL reaction mixture containing 750 µL of the first-step solution, 2 mM NADH, 0.11 mM NsTDH, 0.14 mM BsMDH and 170, 220, 280, or 380 mM isopropanol in potassium phosphate buffer was prepared and used in the second step, which was carried out for 12 h.

phenomenon was likely attributed to the inactivation of enzymes in the presence of a high concentration of methanol.

Finally, we tested the incorporation of the BsMDH/isopropanol system for NADH recycling in the synthesis of L-threitol from formaldehyde. At 900 mM, 1200 mM, 1500 mM, and 2100 mM formaldehyde (the final concentration in the first step), 138.8 mM, 192.8 mM, 251.3 mM and 312.3 mM of L-threitol were produced, respectively. The yield reached 82.3%, 85.7%, 89.4%, and 79.3% (Fig. 6B). When using the BsMDH/isopropanol NADH regeneration system, the consumption and production of L-erythrulose were balanced in the L-threitol synthesis route (Fig. 6A), leading to much less accumulation of the intermediate L-erythrulose compared to the other two systems. In this system, isopropanol was converted to acetone, which could be easily removed and recycled from the reaction system by evaporation. This reaction route allowed maximizing the substrate conversion and minimizing the product purification steps. To further investigate the scalability of the cascade reaction, the reaction volume was increased to 45 mL for the first step and 50 mL for the second step. As shown in Fig. S5,† 157.2 mM L-threitol was obtained, corresponding to a yield of 55.9%, which is lower than the

yield of the 1 mL-scale reaction. For the first step, it was found that 248 mM L-erythrulose was produced. When the reaction solution of the first step was added to the second step, the concentration of L-erythrulose became 186 mM, and 157.2 mM L-threitol was produced, which led to 84.5% yield for the second step. Therefore, further investigation and optimization for the scale-up reaction is required in the future, especially for the first step. This result highlights the potential of the multi-enzymatic system for L-threitol production.

Among the three NADH regeneration systems, the GldA/glycerol system enabled the highest production of L-threitol (405.69 mM) but with a side product, L-erythrulose (up to 138.9 mM), while the BsMDH/isopropanol system resulted in the second-highest production of L-threitol (312.3 mM) but with a negligible amount of side product L-erythrulose, which will require less purification effort and thereby reduce the cost. Furthermore, the GldA/glycerol system requires 2.6 times the amount of substrate (glycerol) than the BsMDH/isopropanol

system (isopropanol). Therefore, from the techno-economic analysis point of view, the BsMDH/isopropanol system is likely to have more potential for NADH recycling.

Conclusions

In summary, the first synthesis route of L-threitol from formaldehyde has been presented in this study. The study also provided a new route for the utilization of C1 compounds. Formolase and fructose-6-phosphate aldolase efficiently catalysed the conversion of formaldehyde to L-erythrulose, while L-threitol dehydrogenase facilitated the conversion of L-erythrulose into L-threitol. The implemented NADH regeneration system ensured efficient coenzyme recycling. L-Threitol was produced with a very low amount of side product. This study opens up the possibility for the sustainable production of L-threitol and highlights the potential of enzymatic cascade reactions in the synthesis of valuable compounds from C1 compounds. Enzymatic transformation of cost-effective formaldehyde represents an attractive approach for the synthesis of L-threitol.

Author contributions

S. G. and T. L. contributed equally to this work. S. G. and T. L. designed and optimized the reaction routes. Z. Tan, R. Z. and Z. Tang performed enzyme expression and purification. L. Z. and H. L. conceived and designed the overall experiments. The draft of the manuscript was mainly written by S. G., T. L. and Z. Tan. L. Z. and K. O. supervised the project. L. Z. finally approved the current version.

Data availability

The data supporting this article have been included as part of the ESI.†

Conflicts of interest

There are no conflicts to declare.

Acknowledgements

References

1 H. Wiendl, B. C. Kieseier, R. Weissert, H. A. Mylius, U. Pichlmeier, H. P. Hartung, A. Melms, W. Kuker and M. Weller, *J. Neurol.*, 2007, **254**, 884–889.

2 G. Bemis, R. Parvin and P. Chaturvedi, US5763488A, 1999.

3 R. Kaur, J. Chen, A. Dawoodji, V. Cerundolo, Y. R. Garcia-Diaz, J. Wojno, L. R. Cox, G. S. Besra, B. Moghaddam and Y. Perrie, *J. Pharm. Sci.*, 2011, **100**, 2724–2733.

4 M. M. Gruza, A. Pokrop and J. Jurczak, *Tetrahedron: Asymmetry*, 2005, **16**, 1939–1946.

5 B. Meier, M. Kollroser and A. Presser, *Monatsh. Chem.*, 2014, **145**, 305–309.

6 M. C. Feiters, R. J. M. Nolte and B. Zwanenburg, *Recl. Trav. Chim. Pays-Bas*, 1994, **113**, 194–200.

7 A. Mills, K. Lawrie, J. Bardin, A. Apedaile, G. A. Skinner and C. O'Rourke, *Analyst*, 2012, **137**, 106–112.

8 C. Y. Park, B. M. Kim and K. B. Sharpless, *Tetrahedron Lett.*, 1991, **32**, 1003–1006.

9 J. Kofoed, J.-L. Reymond and T. Darbre, *Org. Biomol. Chem.*, 2005, **3**, 1850–1855.

10 E. Myriam, W. W. R. Harald, H. F. B. Roland and M. J. C. Sonia, US 5756865A, 1998.

11 R. D. Batt, F. Dickens and D. H. Williamson, *Biochem. J.*, 1960, **77**, 272–281.

12 S. Endo, T. Matsunaga, T. Kuragano, S. Ohno, Y. Kitade, K. Tajima, O. El-Kabbani and A. Hara, *Arch. Biochem. Biophys.*, 2010, **503**, 230–237.

13 T. Li, Z. Tang, H. Wei, Z. Tan, P. Liu, J. Li, Y. Zheng, J. Lin, W. Liu, H. Jiang, H. Liu, L. Zhu and Y. Ma, *Green Chem.*, 2020, **22**, 6809–6814.

14 T. Li, Z. Tan, Z. Tang, P. Liu, H. Liu, L. Zhu and Y. Ma, *Green Chem.*, 2022, **24**, 5064–5069.

15 J. Yang, S. Sun, Y. Men, Y. Zeng, Y. Zhu, Y. Sun and Y. Ma, *Catal. Sci. Technol.*, 2017, **7**, 3459–3463.

16 J. A. Castillo, C. Guérard-Hélaine, M. Gutiérrez, X. Garrabou, M. Sancelme, M. Schürmann, T. Inoue, V. Hélaine, F. Charmantray, T. Gefflaut, L. Hecquet, J. Joglar, P. Clapés, G. A. Sprenger and M. Lemaire, *Adv. Synth. Catal.*, 2010, **352**, 1039–1046.

17 H. Huang, M. S. Carter, M. W. Vetting, N. Al-Obaidi, Y. Patskovsky, S. C. Almo and J. A. Gerlt, *J. Am. Chem. Soc.*, 2015, **137**, 14570–14573.

18 H. Jiang, W. Ding, Y. Liu and Y. Yang, CN201711462800.5, 2017.

19 V. Truniger and W. Boos, *J. Bacteriol.*, 1994, **176**, 1796–1800.

20 W. B. Whitaker, J. A. Jones, R. K. Bennett, J. E. Gonzalez, V. R. Vernacchio, S. M. Collins, M. A. Palmer, S. Schmidt, M. R. Antoniewicz, M. A. Koffas and E. T. Papoutsakis, *Metab. Eng.*, 2017, **39**, 49–59.